Annu. Rev. Fluid Mech. 2002. 34:349–74

WALL-LAYER MODELS FOR LARGE-EDDY SIMULATIONS

Ugo Piomelli and Elias Balaras
Department of Mechanical Engineering, University of Maryland, College Park, Maryland 20742; e-mail: ugo@eng.umd.edu, balaras@eng.umd.edu

Key Words large-eddy simulations, wall-layer models, approximate boundary conditions

■ **Abstract** Because the cost of large-eddy simulations (LES) of wall-bounded flows that resolve all the important eddies depends strongly on the Reynolds number, methods to bypass the wall layer are required to perform high-Reynolds-number LES at a reasonable cost. In this paper the available methodologies are reviewed, and their ranges of applicability are highlighted. Various unresolved issues in wall-layer modeling are presented, mostly in the context of engineering applications.

1. INTRODUCTION

The decrease in the cost of computer power over the last few years has increased the impact of computational fluid dynamics. Numerical simulations of fluid flows, which until a few decades ago were confined to the research environment, are now successfully used for the development and design of engineering devices. Despite the advances in computer speed and the algorithmic developments, however, the numerical simulation of turbulent flows has not yet reached a mature stage: None of the techniques currently available can be reliably applied to all problems of scientific or technological interest.

The solution of the Reynolds-averaged Navier-Stokes equations (RANS) is the tool that is most commonly applied, especially in engineering applications, to the solution of turbulent flow problems. The RANS equations are obtained by time- or ensemble-averaging the Navier-Stokes equations to yield a set of transport equations for the averaged momentum. The effect of all the scales of motion is modeled. Models for the RANS equations have been the object of much study over the last 30 years, but no model has emerged that gives accurate results in all flows without ad hoc adjustments of the model constants (see Wilcox 2001). This may be due to the fact that the large, energy-carrying eddies are much affected by the boundary conditions, and universal models that account for their dynamics may be impossible to develop.

0066-4189/02/0115-0349$14.00

In direct numerical simulations (DNS), on the other hand, all the scales of motion are resolved accurately, and no modeling is used. DNS is the most accurate numerical method available at present but is limited by its cost: Because all scales of motion must be resolved, the number of grid points in each direction is proportional to the ratio between the largest and the smallest eddy in the flow. This ratio is proportional to $Re_L^{3/4}$ (where Re_L is the Reynolds number based on an integral scale of the flow). Thus, the number of points in three dimensions is $N_x N_y N_z \propto Re_L^{9/4}$. Present computer resources limit the application of DNS to flows with $Re_L = o(10^4)$, and the $Re_L^{3/4}$ dependence of the number of grid points makes it unrealistic to expect that DNS can be used for high-*Re* engineering applications in the near future. A recent review of DNS can be found in Moin & Mahesh (1998).

Large-eddy simulation is a technique intermediate between the solution of the RANS equations and DNS. In large-eddy simulation (LES) the large, energy-carrying eddies are computed, whereas only the small, subgrid scales of motion are modeled. LES can be more accurate than the RANS approach because the small scales tend to be more isotropic and homogeneous than the large ones, and thus more amenable to universal modeling. Furthermore, the modeled subgrid scale (SGS) stresses only contribute a small fraction of the total turbulent stresses. Compared with DNS, LES does not suffer from the same strict resolution requirements of DNS. Recent reviews of LES can be found in the articles by Mason (1994), Lesieur & Métais (1996), Piomelli (1999), and Meneveau & Katz (2000).

LES has received increased attention, in recent years, as a tool to study the physics of turbulence in flows at higher Reynolds number, or in more complex geometries, than DNS. Its most successful applications, however, have still been for moderate Reynolds numbers; examples include the flow inside an internal combustion engine (Verzicco et al. 2000) or the sound emission from the trailing edge of a hydrofoil at $Re_c = 2 \times 10^6$ (Wang & Moin 2000). In a wide range of flows in the geophysical sciences (especially in meteorology and oceanography) and engineering (for instance, in ship hydrodynamics or in aircraft aerodynamics), however, the Reynolds number is very high, of the order of tens or hundreds of millions. The extension of LES that resolves the wall-layer structures (henceforth called "resolved LES") to such flows has been less successful owing to the increased cost of the calculations when a solid boundary is present.

The first complete analysis of grid-resolution requirements for LES of turbulent boundary layers can be found in the landmark paper by Chapman (1979). The flow in a flat-plate boundary layer or plane channel is generally divided into an inner layer in which the effects of viscosity are important and an outer one in which the direct effects of the viscosity on the mean velocity are negligible. Chapman (1979) examined the resolution requirements for inner and outer layers separately. In the outer layer in which the important eddies scale like the boundary-layer thickness or the channel half-height δ, he obtained an estimate for the outer-layer resolution by integrating Pao's (1965) energy spectrum and showed that the number of points in the wall-normal direction required to resolve a given fraction of the turbulent kinetic energy is essentially independent of *Re*. Assuming that the grid size in

the streamwise and spanwise directions is a fixed fraction of the boundary-layer thickness (which varies approximately like $Re^{0.2}$) his estimate results in a total number of grid points proportional to $Re^{0.4}$. Chapman estimated that only 2500 points are required to resolve a volume $\overline{\delta}^3$ of the flow, where $\overline{\delta}$ is an average boundary-layer thickness. In actual calculations a wide range of resolutions is found: In calculations of plane channel flow, for instance, Schumann (1979) used between 128 and 4096 points to resolve a volume δ^3 (here δ is the channel half-height), whereas Piomelli et al. (1989) used 1000 points.

The resolution of the inner layer is much more demanding: Its dynamics are dominated by quasi-streamwise vortices (see the review by Robinson 1991) whose dimensions are constant in wall units (i.e., when normalized with the kinematic viscosity ν and the friction velocity $u_\tau = (\tau_w/\rho)^{1/2}$, where τ_w is the wall stress and ρ the fluid density). If the inner-layer eddies are resolved, a constant grid spacing in wall units must be used. In a boundary layer or channel flow, this requirement results in streamwise and spanwise grid sizes $\Delta x^+ \simeq 100$, $\Delta z^+ \simeq 20$ (where wall units are defined as $x_i^+ = x_i u_\tau/\nu$). As the outer flow is approached, however, larger grid spacings can be used. An optimal computation, therefore, would use nested grids, with Δx^+ and Δz^+ increasing as one moves away from the wall. Under these conditions, Chapman (1979) estimated that the number of points required to resolve the viscous sublayer is

$$(N_x N_y N_z)_{vs} \propto C_f Re_L^2, \tag{1}$$

which, assuming $C_f \propto Re_L^{-0.2}$, gives

$$(N_x N_y N_z)_{vs} \propto Re_L^{1.8}. \tag{2}$$

In plane channel flow (an important test case for numerical simulations) Chapman's (1979) estimate for the cost of the outer layer needs to be modified. The size of the largest eddies is determined by the channel height and is not a function of the Reynolds number, whereas the cost of resolving the inner layer is the same for channels and boundary layers. Grid-resolution estimates for more complex flows cannot be derived a priori.

Using the estimates for boundary-layer flows, Figure 1 shows that at $Re_L = o(10^6)$, 99% of the points are used to resolve an inner layer whose thickness is only 10% of the boundary layer. As a consequence, the number of points required by LES if the inner layer is resolved exceeds present computational capabilities already at moderate Reynolds numbers.

To estimate the cost of the calculation, one must consider that the equations of motion must be integrated for a time proportional to the integral timescale of the flow, with a time step limited by the need to resolve the life of the smallest eddy. Reynolds (1990) estimates the cost by assuming that the operation count scales like the number of points and that the time step be determined by the timescale of the smallest eddy, which is inversely proportional to its length scale and, therefore, to the grid size. This gives a number of time steps proportional to $(N_x N_y N_z)^{1/3}$ and

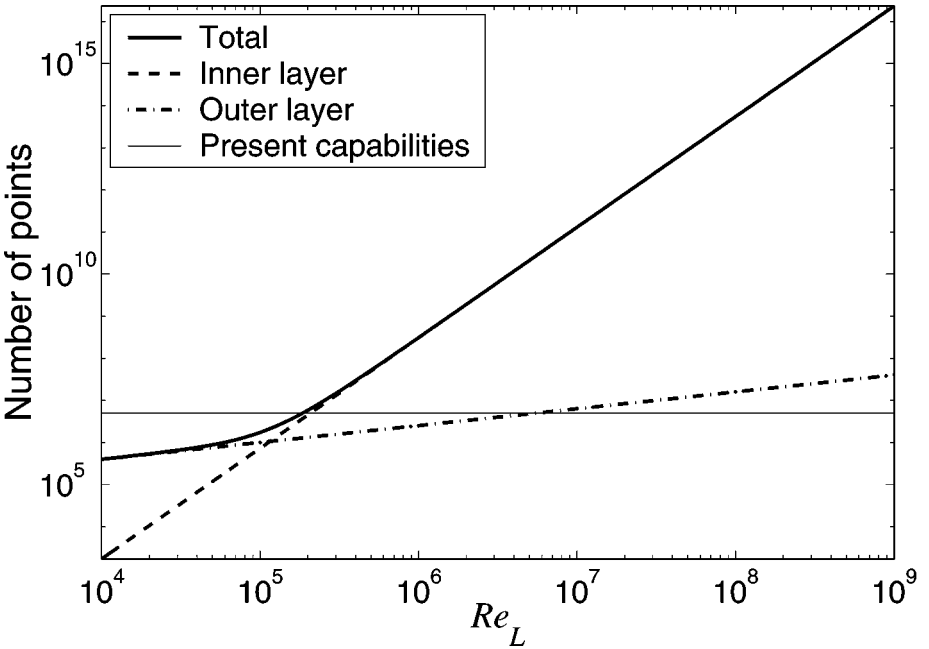

Figure 1 Number of grid points required to resolve a boundary layer. The "Present capabilities" line represents calculations performed on a Pentium III 933MHz workstation with 1Gbyte of memory.

a total cost that is proportional to $(N_x N_y N_z)^{4/3}$. This estimate gives a cost that scales like $Re^{0.5}$ for the outer layer, and $Re^{2.4}$ for the inner one. This estimate disregards the viscous stability conditions and is strictly valid only for calculations in which at least the diffusion is treated implicitly, or neglected.

The only economical way to perform LES of high Reynolds-number attached flows, therefore, is by computing the outer layer only. The grid size can, under these conditions, be determined by the outer-flow eddies, and the cost of the calculation becomes only weakly dependent on the Reynolds number. Because the grid is too coarse to resolve the inner-layer structures, the effect of the wall layer must be modeled. In particular, the momentum flux at the wall (i.e., the wall stress) cannot be evaluated by discrete differentiation because the grid cannot resolve either the sharp velocity gradients in the inner layer or the quasi-streamwise and hairpin vortices that transfer momentum in this region of the flow. Therefore, some phenomenological relation must be found to relate the wall stress to the outer-layer flow.

This requirement spurred the development of models for the wall layer, also known as approximate boundary-conditions. Wall-layer models were initially developed along parallel lines by geophysical scientists and engineers. The principal

difference between the two fields is the presence of stratification, which is important in meteorological flows but usually not in engineering. Stratification effects are not treated in the present review, which concentrates on the engineering applications and development and only briefly outlines the models used by geophysical scientists and meteorologists.

In the following, first the basic philosophy of wall-layer modeling is laid out, and the assumptions and approximations common to most of the methods proposed in the literature are discussed. Then, in Sections 2.1–3, a review of the various approaches that have appeared in the literature is carried out. This is followed by a discussion of other sources of errors that may appear in calculations in which only the outer layer is computed. Some conclusions are drawn in Section 4.

2. WALL-LAYER MODELING

Most wall-layer models, explicitly or implicitly, consider the inner layer in a Reynolds-averaged sense. If the grid is so coarse that it contains a large number of eddies, as illustrated in Figure 2, only their average effect must be represented by the wall-layer model. From one time step to the next, the grid cell adjacent to the wall sees a large number of near-wall eddies that go through several life cycles because their timescale is smaller than the time step, usually determined by outer-flow numerical stability conditions. If the sample of near-wall eddies in a grid cell is large enough, the inner layer can be assumed to be governed by the Reynolds-averaged Navier-Stokes equations, rather than the filtered Navier-Stokes equations solved in LES in the outer layer, and statistical arguments can be used.

For this assumption to hold, the grid size must be very large: In plane channel flow, the grid size must be of the order of 1500 wall units in the streamwise direction and 700 in the spanwise direction. In this case the root-mean-square of the difference between the instantaneous velocity profiles and the logarithmic law would be less than 10%. As a consequence of this requirement, if the grid is too fine ($\Delta x^+ \simeq 100 - 200$, $\Delta z^+ \simeq 50 - 100$), the statistical considerations on which wall-layer models are based fail. Secondly, if the grid is coarse in the plane parallel to the wall ($\Delta x^+ > 1000$, $\Delta z^+ > 500$), but the first point is fairly close to the wall (say, at $y^+ < 50$), the grid cannot resolve the turbulent eddies present in this region of the flow. This may result in aliasing errors that corrupt the velocity field. These two issues may explain why wall-layer models tend to be more accurate at very high Reynolds numbers (in which the grids are necessarily coarse in all directions) than at low or moderate ones.

Validation of LES with wall models can be performed by comparison with experiments or with resolved LES or DNS data. The latter has the advantage that the boundary conditions can be matched exactly, and numerical and SGS modeling errors can be separated (to some extent) from those due to the approximate boundary conditions. However, SGS and numerical errors in the resolved LES are

usually largest in the near-wall layer; thus it is conceivable that calculations that use "perfect" wall-layer models could give more accurate predictions than resolved ones. Furthermore, the Reynolds number achievable by resolved LES and DNS, as mentioned above, is quite low; this can affect the accuracy of the wall models. High Reynolds-number experimental data is more easily available, but it is more difficult to reproduce the experimental setup accurately, and differences between calculations and experimental data are often due to differences in the boundary conditions (see, for example, the discussion in Kaltenbach et al. 1999) as well as to numerical and modeling errors.

The simplest approach to relate the wall stress to the outer velocity is to neglect all terms in the streamwise momentum equation except the Reynolds-stress gradient. This implies that the acceleration and pressure gradient at the first grid point are negligible and that the first grid point is far enough from the wall that viscous effects are negligible. If, in addition, the shear stress is assumed to be constant between the wall and the first point, one can derive a logarithmic velocity profile in the inner layer either of the form

$$u^+ = \frac{u}{u_\tau} = \frac{1}{\kappa} \log y^+ + B, \tag{3}$$

where κ is the von Kármán constant, or

$$u^+ = \frac{1}{\kappa} \log \frac{y}{y_o}, \tag{4}$$

where y_o is the roughness height. This profile can be used to obtain the wall stress given the velocity (obtained from the outer-flow calculation) at the first grid point. The details of this approach are discussed in Section 2.1.

More recently, zonal approaches in which the RANS equations are solved in the inner layer have been proposed and tested to remove those limiting assumptions. They are described in Section 2.2. Other methods are discussed in the final subsection.

2.1. Equilibrium Laws

The limitations of LES, when applied to wall-bounded flows, were recognized in the very early stages of the development of the technique: In the ground-breaking LES of plane channels and annuli by Deardorff (1970) and Schumann (1975), respectively, approximate wall-boundary conditions were introduced to model the effect of the wall layer, which could not be resolved with the computer power available at that time even at moderate Reynolds numbers. In the methodology they proposed, information from the outer flow is used to determine the local wall stress, which is then fed back to the outer LES in the form of the proper momentum flux at the wall due to normal diffusion. The no-transpiration condition was used on the wall-normal velocity component. Today this general approach is still in use in various forms. The cost of these calculations is due to the outer-layer computation only and is proportional to $Re^{0.5}$ for spatially developing flows.

Deardorff (1970), in his channel flow computations, restricted the second derivatives of the velocity at the first off-wall grid point to be

$$\frac{\partial^2 \bar{u}}{\partial y^2} = -\frac{1}{\kappa Y^2} + \frac{\partial^2 \bar{u}}{\partial z^2}, \tag{5}$$

$$\frac{\partial^2 \bar{w}}{\partial y^2} = \frac{\partial^2 \bar{w}}{\partial x^2}, \tag{6}$$

where x indicates the streamwise direction, z the spanwise direction, and y the wall-normal direction; u, v, and w are the velocity components in the three coordinate directions, respectively, and an overbar denotes a filtered (or large-scale) quantity. Y is the location of the first point away from the wall. Equation 5 forces the plane-averaged velocity profile to satisfy a logarithmic law in the mean at point Y. All quantities in Equations 5 and 6 are normalized by u_τ and v.

The results obtained by Deardorff (1970) for the turbulent channel flow at infinite Reynolds number do not compare well with the experimental data of Laufer (1950). The wall model, however, most likely has a small contribution to these errors, which are mainly due to the resolution in the outer layer that was not sufficient to resolve the large energy-carrying structures. A total of 6720 grid nodes were used, which corresponds to approximately 400 points to resolve a volume δ^3; this is six times less than the number of required points estimated by Chapman (1979). When using an alternative set of boundary conditions proposed in the same paper, which essentially implies that the logarithmic law (Equation 4) holds locally, no difference was observed in the statistics.

Schumann (1975) used conditions that directly relate the shear stresses at the wall, $\tau_{xy,w}$ and $\tau_{yz,w}$, to the velocity in the core by

$$\tau_{xy,w}(x, z) = \frac{\langle \tau_w \rangle}{\langle \bar{u}(x, Y, z) \rangle} \bar{u}(x, Y, z), \tag{7}$$

$$\tau_{yz,w}(x, z) = \nu \frac{\bar{w}(x, Y, z)}{Y}, \tag{8}$$

where $\langle \cdot \rangle$ denotes averaging over a plane parallel to the solid wall. The mean stress $\langle \tau_w \rangle$ is assigned a value equal to the given pressure gradient, or it can be calculated iteratively using Newton iterations and requiring that the plane-averaged velocity at the first grid point, $\langle \bar{u}(x, Y, z) \rangle$, satisfy the logarithmic law (Equation 4) at point Y. In phase with the adjacent local outer velocity, the resultant streamwise component (τ_{xy}) of local wall-stress fluctuates around the mean value. The spanwise component (τ_{yz}) is obtained by assuming a linear velocity profile and a constant-eddy viscosity in the grid cell adjacent to the wall. The channel-flow computations carried out in this study gave results in very good agreement with the reference experimental data. Given the poor agreement with experiments in Deardorff's (1970) simulations (discussed above) this series of computations was essentially the first to demonstrate the feasibility of LES using approximate

wall-boundary conditions. In a later study Grötzbach (1987) used a similar approach to assign the wall-heat flux in calculations of turbulent flows with heat transfer and obtained favorable results.

Piomelli et al. (1989) applied conditions similar to Equations 7 and 8. However, to take into account the inclination of the elongated structures in the near-wall region, they required that the wall stress be correlated to the instantaneous velocity some distance downstream of the point where the wall stress is required:

$$\tau_{xy,w} = \frac{\langle \tau_w \rangle}{\langle \bar{u}(x, Y, z) \rangle} \bar{u}(x + \Delta_s, Y, z), \tag{9}$$

$$\tau_{yz,w} = \frac{\langle \tau_w \rangle}{\langle \bar{u}(x, Y, z) \rangle} \bar{w}(x + \Delta_s, Y, z), \tag{10}$$

where Δ_s is a streamwise displacement; its optimum value can be obtained from DNS or experimental data and is approximately $\Delta_s = Y \cot 8^\circ$ for $30 < Y^+ < 50$, and $\Delta_s = Y \cot 13^\circ$ for larger distances for the range of Reynolds numbers investigated. The plane-averaged wall stress is obtained by iterative solution of Equation 3 as in the Schumann (1975) model above. These changes yielded improved results with respect to the original formulation and were used by Balaras et al. (1995) to study the flow in a plane channel for a range of Reynolds numbers in conjunction with the dynamic SGS model, with results in excellent agreement with experimental and DNS data.

All the above approximate boundary conditions are applicable to geometrically simple flows in which the mean wall stress can be obtained from some form of the law-of-the-wall. Extension to more complex configurations is possible only if the mean wall stress can be specified. Wu & Squires (1998) performed LES of a three-dimensional boundary layer over a swept bump using an approach similar to that of Schumann (1975): Equations 7 and 8 were used, with the mean wall stress obtained from a separate RANS calculation. The mean velocity in these equations was computed by performing spanwise averages at each time step during the calculation. Their results are in fairly good agreement with the reference experimental data. This type of approach could be useful in some cases in which RANS simulations or prior experimental studies could provide a reasonable estimate of the mean wall stress, but extension to complex flows is impractical because it relies on the accuracy of the RANS approach.

Most of the models described above imply that the logarithmic law-of-the-wall holds in the mean: Deardorff (1970) enforced this through the second derivative of the velocity (Equation 5); Schumann (1975) and Piomelli et al. (1989) did so by calculating the mean wall stress from the iterative solution of Equation 3 for u_τ, given $\bar{u}$ at the first grid point off the wall. Alternatively, the logarithmic law can be enforced locally and instantaneously, and the wall stress can be computed by assuming that it is aligned with the outer horizontal velocity, as suggested by Deardorff (1970). This method was extensively tested in a study by Mason & Callen (1986) and is based on local equilibrium of the near-wall region; its validity

strongly depends on the size of the averaging volume (the grid cell), which must contain (as mentioned earlier) a significant sample of inner-layer eddies. In a similar manner Werner & Wengle (1993) fit the local horizontal velocity to a power law matched to a linear profile near the wall to compute the local stress. The results in both cases are not very different from the ones with the other models discussed above.

Although a discussion of the important issues in geophysical calculations is beyond the scope of this paper, it should be mentioned that most wall-layer models used in meteorology are of this type. Moeng (1984), for instance, also computes u_τ by imposing an instantaneous logarithmic law at the first grid point, with a correction for the wall heat flux. A similar relationship is used to evaluate the temperature gradient at the wall (see, for instance, Zhang et al. 1996).

Hoffmann & Benocci (1995) derived an analytical expression for the local stress by integrating analytically the boundary-layer equations coupled with an algebraic turbulence model:

$$\bar{v}_Y = -\frac{d}{dx}\int_0^Y \bar{u}\, dy \tag{11}$$

$$\tau_{xy,w} = \left[\nu_{tot}\frac{\partial \bar{u}}{\partial y}\right]_Y - \bar{u}_Y \bar{v}_Y + \frac{d}{dx}\int_0^Y \bar{u}^2\, dy - Y\frac{dP_e}{dx} - \frac{d}{dt}\int_0^Y \bar{u}\, dy, \tag{12}$$

where ν_{tot} is the total eddy viscosity (sum of molecular and SGS) and dP_e/dx is the external pressure gradient. Hoffman & Benocci (1995) argued that the sum of the two advective terms (the second and third on the right-hand side of Equation 12) can be neglected (they point out that it is not legitimate to neglect only one of them, only their difference). They approximated the unsteady term using a discretized time derivative and order-of-magnitude arguments and modeled the viscous diffusion using κy as the length scale in a mixing-length model. Then, the calculation of the wall stress required only the velocity $\bar{u}_Y$. The results for a channel flow and a rotating channel flow are in good agreement with resolved LES and experimental studies.

The same approach was used by Wang (1999) to calculate the flow over the trailing edge of an airfoil. He examined two cases, one in which only the viscous and turbulent diffusion were used in the equation and one in which the pressure gradient was included. The unsteady term was always neglected. The approximate–boundary condition calculation was in good agreement with the resolved one (Wang & Moin 2000) in the zero or favorable pressure-gradient region (see Figure 3), but the flow in the adverse pressure-gradient region was not predicted accurately. Immediately downstream of the sharp peak in the skin-friction coefficient in Figure 3, the wall model does not respond correctly to the transition from the favorable to the adverse pressure gradient. The frequency spectra of

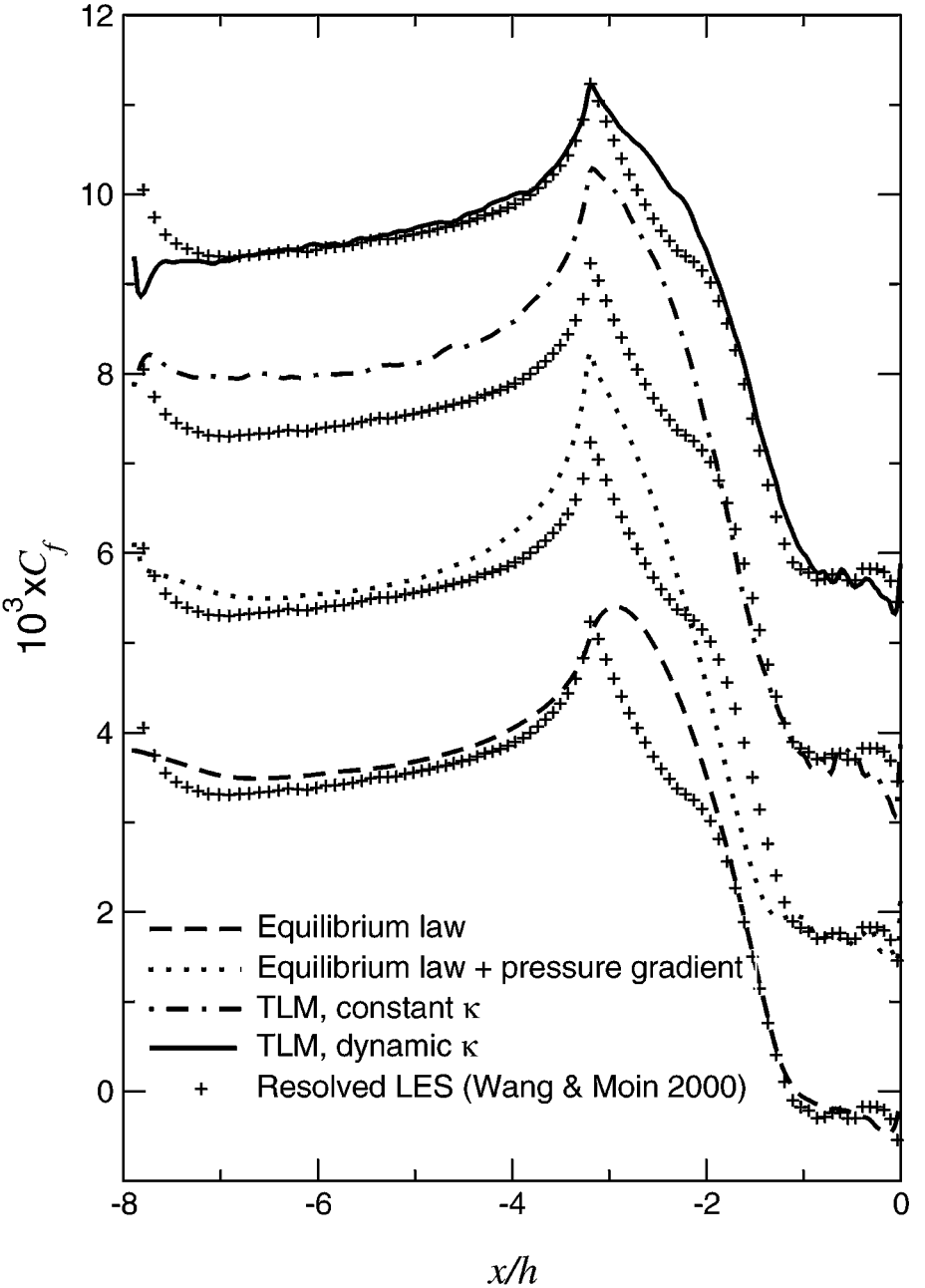

Figure 3 Distribution of the skin-friction coefficient near the trailing edge on the top surface of the airfoil. Each set of curves is shifted by two units in the vertical direction. The calculations that use the TLM approach are discussed in Section 2.2. Data from Wang (2000).

wall-pressure fluctuations agree well with those obtained from the resolved calculation, except in the adverse pressure-gradient and separated regions. Wang (1999) also computed the far-field noise generated by the sharp trailing edge and found that the predictions of the calculations with approximate boundary conditions did not match the resolved ones in the frequency range associated with scales generated in the separation region, whereas at other frequencies the agreement was acceptable.

2.2. Zonal Approaches

Zonal approaches are based on the explicit solution of a different set of equations in the inner layer. There are two approaches: In one, known as the Two-Layer Model (TLM), two separate grids are used. In the other, which is based on the Detached Eddy Simulation method proposed by Spalart et al. (1997), a single grid is used, and only the turbulence model changes.

The TLM was proposed by Balaras & Benocci (1994) and was extensively tested in a follow-up paper by Balaras et al. (1996). Whereas the filtered Navier-Stokes equations are solved in the core of the flow, in the wall layer a simplified set of equations is solved in a grid that is refined in the wall-normal direction only and is embedded in the coarser LES mesh (see Figure 4). The basic assumption behind this technique is that the interaction between the near-wall region and the outer region is weak. The TLM uses the boundary-layer equations in the inner layer:

$$\frac{\partial \bar{u}_i}{\partial t} + \frac{\partial}{\partial x_i}(\bar{u}_n \bar{u}_i) = -\frac{\partial \bar{p}}{\partial x_i} + \frac{\partial}{\partial x_n}\left[(\nu + \nu_t)\frac{\partial \bar{u}_i}{\partial x_n}\right], \tag{13}$$

where n indicates the normal direction and i spans 1,2 or 1,3 depending on whether the wall plane is the $x - y$ or $x - z$ plane. The unknown normal velocity u_n is computed by imposing mass conservation in the inner layer. The inner-layer flow is calculated by integrating Equation 13 using the no-slip condition at the wall, and the velocity at the first grid point is obtained from the outer-flow LES as a

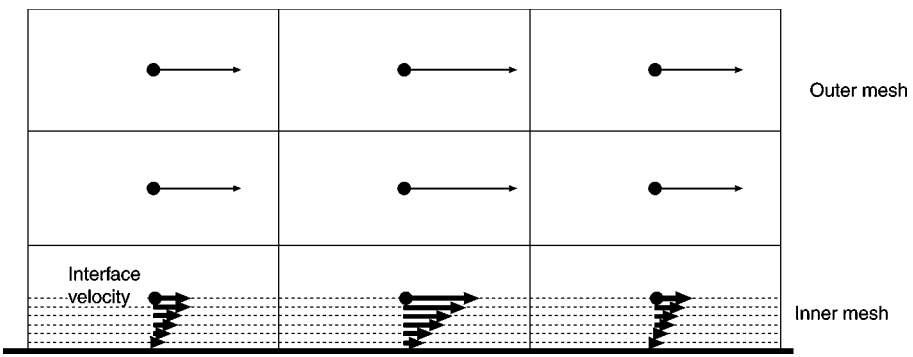

Figure 4 Inner-and outer-layer grids for the two-layer model.

"freestream" condition. The wall-stress components obtained from the integration of Equation 13 in the inner layer are then used as boundary conditions for the outer-flow calculation.

The cost of this method is marginally higher than the cost of calculations that use equilibrium boundary-conditions because the inner layer requires a small percentage of the total cost of the calculation. Two one-dimensional problems are solved, and no Poisson-equation inversion is required to obtain the pressure.

In Balaras & Benocci (1994) and Balaras et al. (1996) an algebraic eddy viscosity model was used to parameterize all scales of motion in the wall layer:

$$\nu_t = (\kappa y)^2 D(y) \left|\bar{S}\right|, \tag{14}$$

where y is the distance from the wall, $\left|\bar{S}\right|$ is the magnitude of the resolved strain-rate tensor, and $D(y)$ is a damping function that assures the correct behavior of ν_t at the wall:

$$D(y) = 1 - \exp[-(y^+/A^+)^3], \tag{15}$$

where $A^+ = 25$.

Balaras et al. (1996) applied the TLM to channel flow for Reynolds numbers $Re_\tau = u_\tau \delta/\nu$ between 200 and 2000, obtaining results in good agreement with resolved LES, DNS, and experiments. The results were also in good agreement with those obtained using the equilibrium-based boundary condition (Equations 9 and 10). Significant improvements over the equilibrium approach were obtained when the TLM was applied to the flow in a square duct and to the flow in a rotating channel. In the square duct the flow in the corners, where a logarithmic law is not valid owing to the secondary flow, was predicted accurately. In the case of the rotating channel the model based on the logarithmic law failed entirely owing to numerical instability introduced by the logarithmic boundary condition. The friction velocity is shown for various rotation numbers $Ro_b = 2\Omega\delta/U_b$ (where U_b is the average velocity in the channel, δ the channel half-height and Ω the rotation rate) in Figure 5. The TLM predictions were in good agreement with the resolved DNS and experiments, even on the stable side of the channel in which significant deviations from the logarithmic profile are observed owing to the tendency toward relaminarization of the flow. The differences observed on the stable side between all the numerical datasets and the experiments are probably due to differences in the flow configurations. In particular, the flow in the experiments may not have been fully developed owing to the short entry length, and the low aspect ratio of the channel may have generated a streamwise pressure gradient that enhanced the tendency of the flow toward relaminarization.

The two-layer model was also the subject of several studies carried out at the Center for Turbulence Research and summarized by Cabot & Moin (1999). In plane channel flow, Cabot (1995) found little difference with the results obtained using the logarithmic law, consistent with the finding of Balaras et al. (1996). Cabot also observed a transition layer in which the mean velocity profile shifts

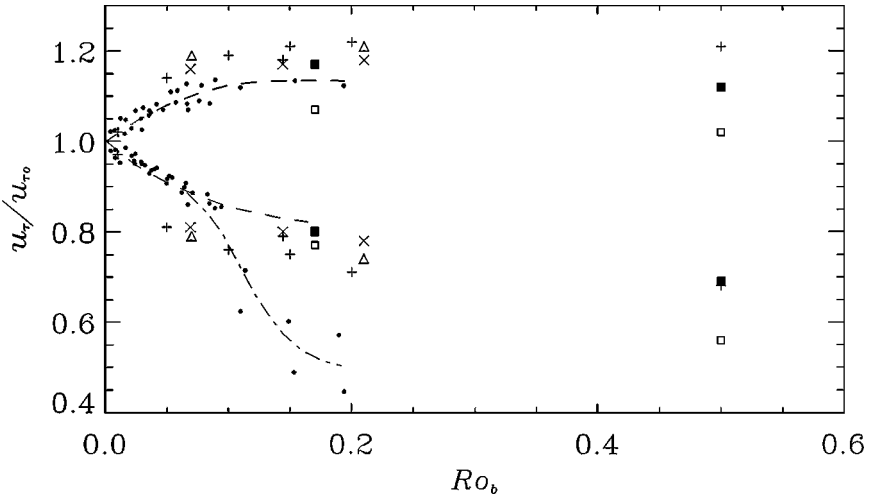

Figure 5 Friction velocity in rotating channel flow. •, Experiments (Johnston et al. 1972); ---, —·—, best fit to experimental data (Johnston et al. 1972); +, DNS (Kristoffersen & Andersson 1993); ■, DNS (Lamballais et al. 1998); □ resolved LES (Lamballais et al. 1998); ×, resolved LES (Piomelli & Liu 1995); △, LES with wall models (Balaras et al. 1996).

from the imposed logarithmic value at the interface (which corresponds to an intercept $B = 5.5$) to a profile with a lower intercept ($B \simeq 5$) that better fits the experimental data at high Reynolds number (Figure 6). This results in decreased mass flux for a given pressure gradient, but the error is quite small: The maximum velocity is underestimated by approximately 3%.

Cabot (1996) and Diurno et al. (2001) applied the TLM to the calculation of a backward-facing step for a range of Reynolds numbers. All calculations used second-order accurate staggered schemes for the discretization of the equations of motion and localized versions of the dynamic eddy viscosity model. A variety of inner-layer treatments was used. Cabot (1996) used the configuration shown in Figure 7*a* to compute the flow in a backward-facing step at $Re_h = 28{,}000$ (based on step height and inlet velocity) and with a 4:5 expansion ratio. His configuration and grid were identical to those used by Akselvoll & Moin (1995) for a resolved LES of this flow; downstream of the step, the first 10 grid points in the wall-normal direction were removed, and the TLM was applied. Thus, in the region downstream of the step, $146 \times 97 \times 96$ mesh points were used, only 10% fewer than the resolved calculation. This setup, which does not achieve the computational savings that can be obtained using the TLM, was chosen in order to compare the accuracy of the approach with the resolved calculations eliminating all sources of error apart from the approximate boundary conditions.

The reattachment point obtained by Cabot (1996) was in good agreement with the resolved LE data, although a stronger backflow (compared with the

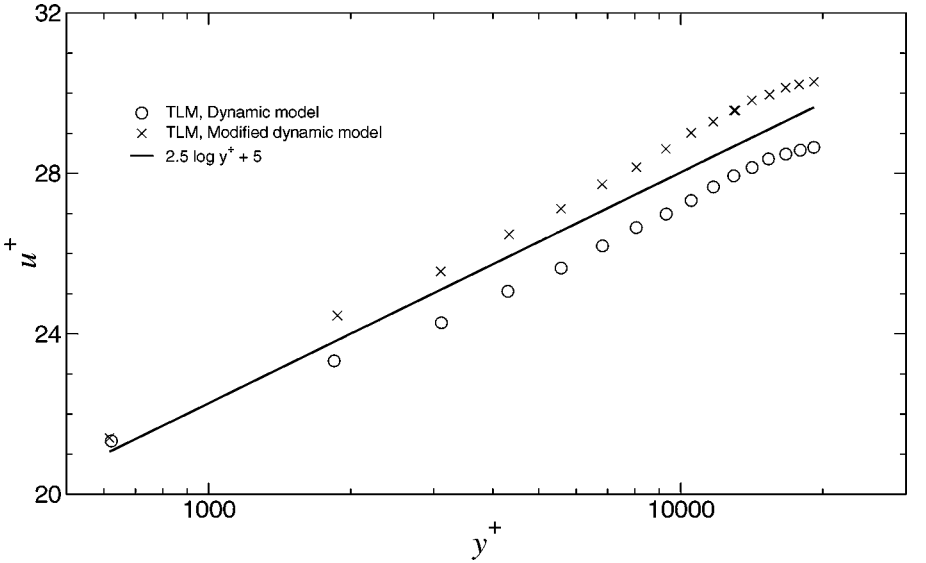

Figure 6 Mean streamwise velocity in wall units for LES with the two-layer model on a 32^3-point mesh at $Re_\tau = 20{,}000$. The modified dynamic model is discussed in Section 3. Data from Cabot & Moin (1999).

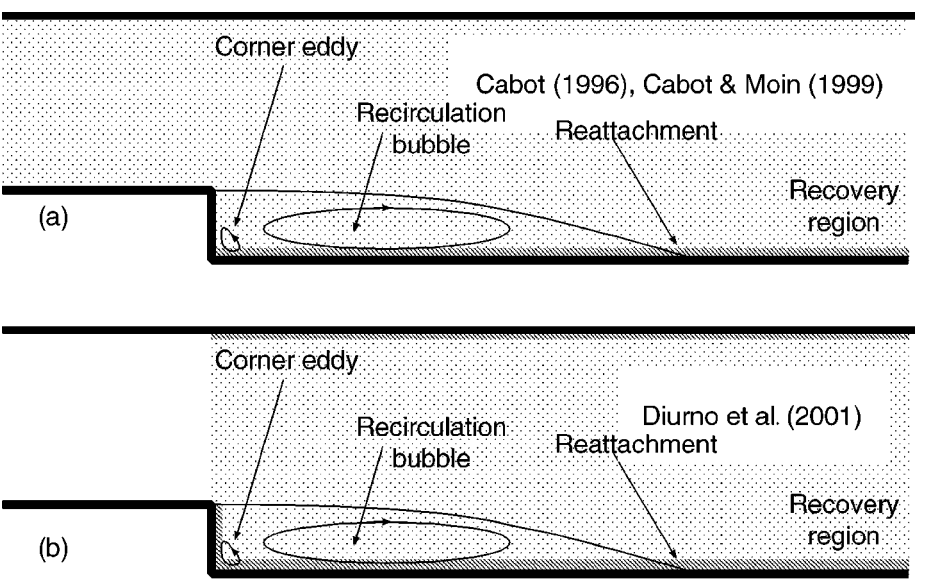

Figure 7 Sketch of the simulation domains used for the backward-facing step calculations. The dotted area indicates the computational domain, the cross-hashed regions the areas in which the wall-layer models were applied. Drawings not to scale.

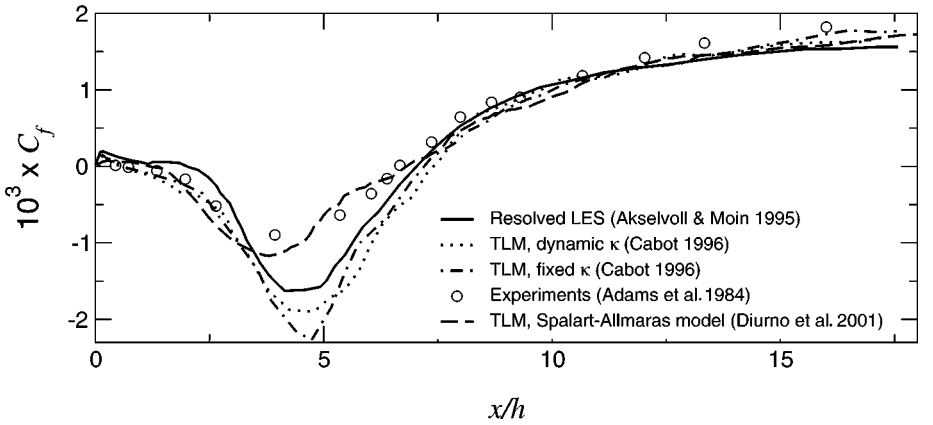

Figure 8 Skin friction coefficient downstream of the step. $Re_h = 28{,}000$.

experimental data) was observed in the recirculating region. This result was consistent with the resolved LES results (Figure 8). No corner eddy was observed. The mean velocity profiles also agreed well with the resolved calculation. Cabot (1996) found that the streamwise pressure term played an important role in the boundary-layer equation for the TLM. He compared the standard mixing-length approach [in which the argument of the exponential in the damping function (Equation 15) was squared, rather than raised to the third power as in Balaras et al. 1996] with a "dynamic" model in which the von Kármán constant κ was modified by forcing the inner-layer eddy viscosity to match (in a least-squares sense) the Reynolds stress predicted in the inner layer with that obtained in the outer flow from the LES. This yielded a lower (by more than a factor of 2) value of the inner-layer viscosity. This modification resulted in a small improvement of the skin-friction prediction in the recirculating region, but otherwise the calculation appeared fairly insensitive to the turbulence model in the inner layer.

Diurno et al. (2001) computed the same flow but used a different configuration, as sketched in Figure 7*b*. They moved the inflow to the corner where they assigned the velocity by using planes of data computed in a separate calculation. They also applied the wall-layer model on all solid surfaces and used $160 \times 80 \times 32$ grid points [one third of the grid points used by Cabot (1996)]; the mesh was stretched near the corner to resolve better the shear layer. They used the standard TLM formulation (Equations 13–15) but also performed calculations in which the eddy viscosity in the inner layer was obtained using the Spalart-Allmaras (1994) turbulence model. The use of a transport equation for the eddy viscosity required the specification of an additional boundary condition. Several implementations were tested, and the one that was found more robust, accurate, and less computationally demanding was to set the inner-layer eddy viscosity equal to the outer-layer SGS eddy viscosity. This boundary condition is justified only if the velocity and its first

derivative are smooth at the interface, which in all computations was true at least in the mean.

Diurno et al. (2001) obtained quite good agreement with the experiments (Figure 8), both with the Spalart-Allmaras (1994) model and with the standard algebraic eddy-viscosity model in the inner layer. They found that the flow field was quite insensitive to the inner-layer treatment, consistent with the results by Cabot (1996). They did observe a secondary recirculating region and a corner eddy that was, however, excessively elongated in the wall-normal direction. Several factors can explain the difference between these results and those obtained by Cabot (1996) using a similar model and numerical scheme. First is the difference in the configuration: Akselvoll & Moin (1995) and Cabot (1996) had a development region upstream of the step in which the grid resolution may not have been sufficient to resolve the boundary layer properly. The wall stress predicted by the LES throughout this region is, in fact, 30% lower than in the experiments. Diurno et al. (2001), on the other hand, had no development region but assigned a boundary layer obtained from a separate calculation that matched the experimental wall stress. Because the state of the boundary layer at the separation point is very important in determining the flow dynamics, this difference can have significant effects. Second, the mesh used by Diurno et al. (2001) near the corner was finer in the streamwise and wall-normal directions compared to that employed by Cabot (1996). Notice that, although Cabot (1996) employed 96 points in this direction, he resolved the wall layer on the upper wall, which was modeled in the computations by Diurno et al. (2001).

In this flow the state of the separating shear layer determines to a very large extent the flow in the separated region. The TLM responds well to outer-flow perturbations; on the other hand, in cases in which the perturbation propagates from the wall, the TLM performance is much less accurate. In Figure 9 the contours of the wall stress in a calculation of the flow at $Re_h = 5{,}100$ illustrate the highly irregular shape of the reattachment line, and the secondary separation bubble, as evidenced by the reversal of the sign of τ_w. The velocity vectors in the separated region (*left plot*) show an attached flow moving toward the corner and the separation due to the corner eddy. Those in the right-hand plot show the attached flow in the recovery region. The fact that the inner layer always sees an attached flow (which may be moving in any direction) explains why the boundary-layer equations are successful in modeling a massively separated flow. If the recirculation bubble were entirely contained within the inner layer and had to be parameterized by the RANS model, the results would probably be less accurate.

Wang (2000) followed his previous work (Wang 1999, described in Section 2.1) by applying the TLM model for the study of the airfoil trailing-edge flow. The results did not improve when the standard inner-layer treatment was used. In fact, the skin-friction coefficient was too high even in the attached region of the flow (Figure 3). He then modified the inner-layer model by using a dynamic constant in the mixing-length expression (Equation 14). The constant was set by requiring that, at the interface, $\nu_t = \nu_T$, where ν_T is the outer-flow SGS eddy viscosity and ν_t is the inner-layer one. This resulted in decreased values of the

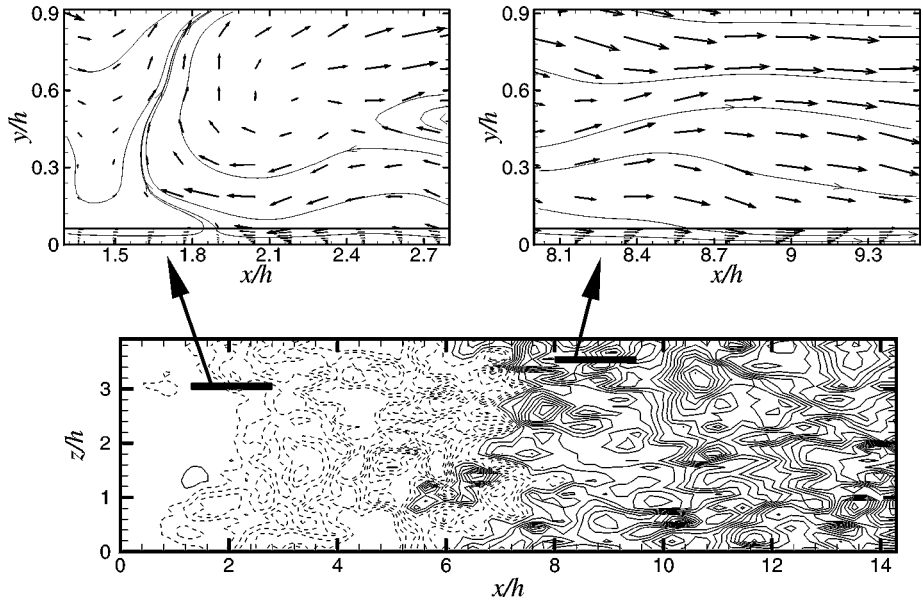

Figure 9 Contours of the instantaneous wall-stress downstream of the step and instantaneous velocity vectors in the $xy-$plane at two locations. The scaling of the vectors on the left-hand-side figure is magnified by a factor of three compared with the right-hand-side. The interface is shown by a thick line and the contour interval is $\Delta\tau_w = 2 \times 10^{-4}$. Dotted contours are negative. $Re_h = 5{,}100$. From Diurno et al. (2001).

inner-layer eddy viscosity (lower by a factor of approximately 3) and in improved agreement with the resolved LES (Figure 3), especially in the adverse pressure-gradient and separated regions. The velocity spectra and the far-field noise were also in better agreement with the resolved case.

Another approach to wall-layer modeling is the Detached Eddy Simulation (DES), introduced by Spalart et al. (1997) as a method to compute massively separated flows. DES is a hybrid approach that combines the solution of the RANS equations in the attached boundary layers with LES in the separated regions in which the detached eddies are important. Recent reviews of the DES formulation and achievements can be found in Spalart (2000) and Strelets (2001). Although DES is not a zonal approach, as it uses a single grid, the turbulence model used separates a RANS region from an LES one, effectively creating two zones, one in which the RANS model has control over the solution and another in which the resolved eddies govern the flow. Notice that, because no zonal interface exists, the velocity field is smooth everywhere. Its original formulation used the Spalart-Allmaras (1994) model, a one-equation model in which a transport equation for the eddy viscosity is solved. By modifying the model length scale to account for the fine resolution in the LES regions, the production of eddy viscosity is decreased far from solid surfaces. When production and destruction are equal, the model

behavior is similar to that of a Smagorinsky (1963) eddy-viscosity model (Strelets 2001). Because the grid size in the plane parallel to the walls scales with the outer-flow eddies, although the first grid point must be at $y^+ \simeq 1$ to ensure accurate calculation of the wall stress by the finite-difference method, the cost of this method compared to a resolved calculation is a weaker function of the Reynolds number. Nikitin et al. (2000) estimate the cost to be proportional to Re_τ, which corresponds roughly to $Re_L^{0.9}$.

In the standard DES approach the entire boundary layer is modeled by RANS. Nikitin et al. (2000), however, used DES as a wall-layer model in calculations of plane channel flow. They performed several calculations with different numerical schemes and grids, exploring a wide range of Reynolds numbers ($180 \leq Re_\tau \leq 80{,}000$). The calculations showed some promising results: Turbulence in the outer layer was sustained even though the flow in the inner layer was smooth owing to the large-eddy viscosity predicted by the Spalart-Allmaras (1994) model. The velocity profiles, shown in Figure 10, have the correct behavior in the inner layer, which is governed by the RANS model, tuned to reproduce the linear and logarithmic

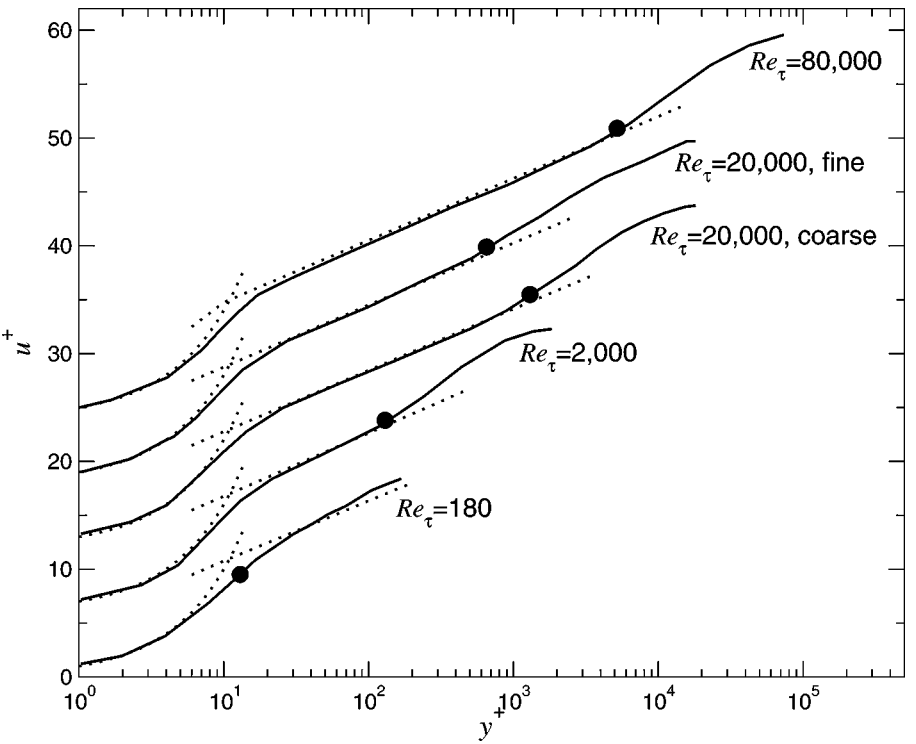

Figure 10 Mean velocity profiles in plane channel flow. DES-based wall-layer model (Nikitin et al. 2000). Each profile is shifted by 6 units in the vertical direction for clarity, and a bullet shows the interface between the RANS and the LES regions.

profiles in flows of this kind. As the flow transitions into the LES region, however, an unphysical "DES buffer layer" is formed in which the velocity gradient is too high. This buffer layer becomes what appears to be an extended wake region, but is instead a logarithmic layer with a high intercept and, in some cases, an incorrect slope. The high intercept is particularly clear in the fine calculation at $Re_\tau = 20{,}000$, in which it extends roughly between $3000 < y^+ < 15{,}000$. When the resolution in the outer LES region was insufficient ($\Delta x = \Delta z = 0.1\delta$), the slope of this spurious logarithmic region was also incorrect. Only at the lowest Reynolds number, in which the grid was fine enough to perform a coarse DNS, were accurate results obtained in the outer layer. These errors were reflected in the skin-friction coefficient, which was underpredicted by approximately 15% in most of the calculations. Although the outer-layer resolution could affect the slope of the logarithmic layer in the LES region, the high intercept must be attributed to other causes because refining the grid in the $Re_\tau = 20{,}000$ calculation did not result in significant improvements.

Because the inner layer was smooth, unphysical, nearly one-dimensional, wall streaks were present in the RANS region, shown in Figure 11, and shorter-scale outer-layer eddies were progressively formed as one moved away from the wall. Baggett (1998) argues that the presence of these artificial streaks causes a decorrelation between u and v fluctuations that must be compensated by a higher velocity gradient to balance streamwise momentum, which shifts the intercept of the LES logarithmic region to a higher value. The mechanism of generation of these artificial streaks is not fully understood. In particular, it is not clear whether they are generated by the nonlinear response of the inner-layer model to outer-flow perturbations or whether the inner layer is forcing the outer flow to have incorrect length scales, thereby causing this transition layer to exist.

In models based on the logarithmic law different results can be observed. Figure 12 shows contours of the vorticity in a channel-flow calculation carried out in a similar configuration (in terms of domain size, grid in the streamwise and spanwise directions) to that used in the DES case. The outer-layer eddies in this case leave a much stronger footprint on the inner layer, which has the same length scales as the outer layer.

2.3. Other Methods

In the methodologies discussed in Sections 2.1 and 2.2 the local wall stress required to impose boundary conditions to the outer LES is computed either from some form of law-of-the-wall or by solving numerically a set of simplified equations. Alternative methods have also been explored over the past years. Bagwell et al. (1993) developed an approach that attempts to incorporate more knowledge of wall-layer coherent structures into wall models. They used the linear stochastic estimate (LSE) approach (Adrian 1979) to obtain the local wall-shear stress given the outer flow. LSE provides the best linear estimate (in the least-squares sense) of the velocity field corresponding to a given "event" (the velocity, strain rate, or pressure at one or more points in the field). Bagwell et al. (1993) assigned an

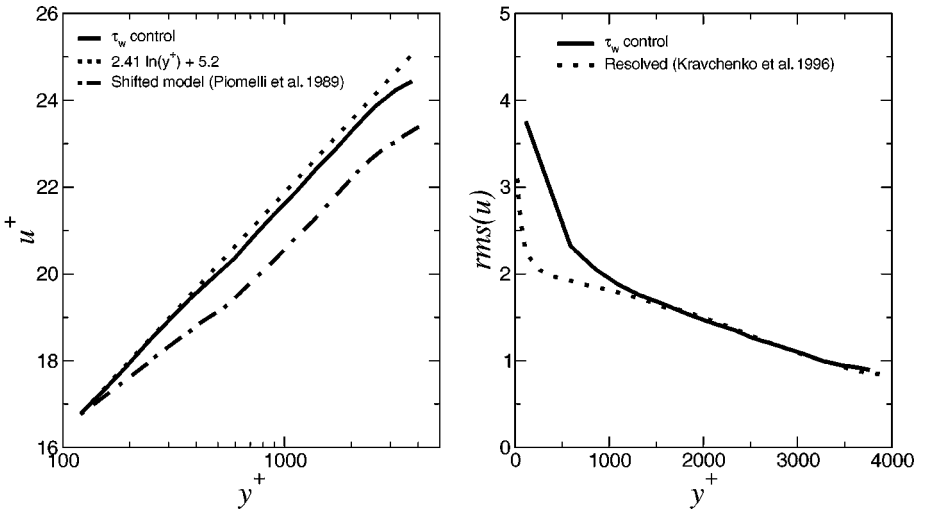

Figure 13 Mean velocity and streamwise turbulence intensity profiles with mean-flow control. Data from Nicoud et al. (2001).

event-field consisting of all velocities on a single horizontal plane adjacent to the wall and obtained results in very good agreement with the DNS data. Even the rms turbulence intensities were predicted accurately down to $y^+ = 15$. The method, however, requires prior knowledge in the form of the two-point spatial correlation tensor, which was taken in this case from DNS data. Although scaling arguments may be invoked to rescale known correlations at different Reynolds numbers (see for example Naguib & Wark 1992), the range of applicability of this approach remains limited.

Nicoud et al. (2001) used suboptimal control theory to supply a wall stress that forced the outer LES to the desired mean velocity profile. This method yielded improved agreement (Figure 13) with the logarithmic law (which was the target profile) but its cost was excessive (approximately 20 times that for the uncontrolled LES). The turbulence intensities were still not predicted accurately in a transition layer near the wall. This indicates that even the specification of the "exact" wall stress may not be sufficient to match the second-order statistics at the inner-outer layer interface, and additional information on the structure of turbulence in this region may be required. To develop a practical model, they coupled the suboptimal-control calculation to the LSE approach. Using the suboptimal-control strategy, they generated a table of outer-flow velocity/wall-stress correlations that, when used as approximate boundary conditions, reproduced the results of the suboptimal-control calculation at a much lower cost. An advantage over similar databases that can be generated from experiments, DNS, or well-resolved LES is that in this case numerical and SGS errors are taken explicitly into account. The LSE model, however, is very sensitive to the numerical scheme employed and to the grid resolution. Baggett et al. (2000) found that the accuracy of the

LSE model deteriorates significantly when the grid is modified or when a different numerical scheme is used than the one employed in the suboptimal-control calculation.

3. OTHER SOURCES OF ERROR

Near the wall, in the outer layer, the dominant eddies become comparable to the grid size, violating the assumptions on which most SGS stress models are based. Furthermore, the accurate evaluation of the strain-rate tensor, which is required by most eddy-viscosity SGS models, may be inaccurate. Finally, the explicit filtering operations commonly used to perform a dynamic evaluation of the model coefficients (Germano et al. 1991) are ill defined near the wall. In addition, numerical errors on the coarse (relative to the size of the dominant eddies) mesh near the wall may be of the same order of magnitude as the divergence of the SGS stress tensor itself.

Cabot et al. (1999) used the dynamic eddy-viscosity model in coarse LES of plane channel flow and compared the standard, dynamic eddy-viscosity model with one in which the dynamic coefficient at the first grid point is obtained from an extrapolation from the flow interior, rather than calculated using local-flow properties. This calculation (shown in Figure 6) yielded a significantly larger eddy viscosity in the outer layer and better agreement with the logarithmic law than the standard approach.

Other approaches that yield improved agreement with experiments and theory on very coarse grids include using a stochastic backscatter model (Mason & Thomson 1992), a two-part model with a contribution that forces directly the mean flow (Schumann 1975, Sullivan et al. 1994), and a scale-dependent, dynamic eddy-viscosity model (Porté-Agel et al. 2000). In this model, a power-law dependence of the dynamic-model coefficient on the filter size is assumed to account for the fact that the dynamic procedure assumes that the explicit filter lies in the inertial region of the spectrum, an assumption usually invalid near the wall in coarse calculations. The optimal-control approach proposed by Nicoud et al. (2001) (discussed above) also tries to correct for modeling and numerical errors explicitly.

4. CONCLUSIONS

Several wall-layer models that have been developed or applied in recent years are described. The state-of-the-art in this area can be summarized by the following points:

1. Simple models work fairly well in simple flows (especially the flows for which they were designed and in which they were calibrated). For instance, models based on the logarithmic law give a fairly accurate prediction of the mean skin-friction coefficient and outer-velocity profile in equilibrium

flows. The Reynolds stresses are also in reasonable agreement with the data outside of a transition layer, a few (two or three) grid-cells thick, in which wall-modeling errors are felt.

2. In more complex configurations in which the flow is driven by the outer layer, equilibrium laws may fail, but zonal models give reasonably accurate predictions. Examples of such flows are the backward-facing step and the airfoil trailing edge. In the first configuration, the mean velocity and skin-friction coefficient were predicted quite accurately, and the transition layer was nearly nonexistent, even in the separated region. In the second one, all the velocity statistics were in good agreement with resolved LES, except in the adverse pressure-gradient region in which the inner-layer model predicts a higher wall stress, whereas the outer-layer velocity profile is not as full as in the resolved calculation. This outer-layer discrepancy might be due to SGS modeling errors.
3. No extensive tests of wall-layer models in complex configurations exist. In nonequilibrium flows in which the inner layer is strongly perturbed, such as, for instance, a three-dimensional shear-driven boundary layer, wall-layer modeling is inaccurate (G.V. Diurno, personal communication). Wall-layer models are not very effective (in the formulations presently in use) at transferring information to the outer layer and tend to be more accurate when the inner/outer-layer interaction is one-way, with the outer layer supplying the forcing.

What level of accuracy can one expect from a "good" wall-layer model? In the authors' opinion, the mean skin-friction coefficient must be predicted accurately, perhaps within 5% of resolved calculations. One should also expect the first- and second-order statistics in the outer layer to be as accurate as in a resolved LES. In plane-channel calculations the turbulent kinetic energy budgets were also found to be in good agreement with resolved LES and DNS data (Balaras et al. 1995), but it is not known whether this objective is achievable in more complex flows.

Present models do not satisfy these requirements. In most cases a transition layer exists (see, for example, Figures 10 and 13) in which the velocity profile switches from the logarithmic law enforced by the inner-layer model to one that the outer-layer satisfies. The transition region is strongly dependent on the type of interaction between inner and outer layer forced by the model used. For instance, in the DES calculations of Nikitin et al. (2000) the intercept of the logarithmic law was too high, whereas in calculations that used the logarithmic law the intercept could be either too high (Piomelli et al. 1989) or too low (Nicoud et al. 2001).

Even in simple flows, there is no a priori reason to expect that the inner-layer logarithmic law enforced, implicitly or explicitly, by most models will match the one established by the resolved calculation in the outer flow. The matching occurs only if both the inner- and outer-layer treatments are accurate (numerical and modeling errors are small) and if their interaction does not introduce spurious

unphysical phenomena. The complex interactions between inner and outer layer, shown in Figures 11 and 12, are affected by many factors: The inner-layer model is only one of them; the outer-flow SGS model, the grid resolution, and the aspect ratio are also important (F. Nicoud, J.S. Bagget, P. Moin, & W.H. Cabot, submitted report).

Several important issues that remain unanswered require attention in order to develop accurate models that work well in a variety of configurations. Progress is being made in SGS modeling on very coarse meshes, an area that has, historically, been of more interest to meteorologists than to engineers. The latter tend to perform very highly resolved calculations in which the integral scale is much larger than the grid or filter size. Better understanding of the interaction between the resolved dynamics in the outer layer and the simplified ones in the inner one is required. Performing well-resolved LES at fairly high Reynolds numbers for model validation is very important. In fact, the use of low Reynolds-number data for this purpose may actually hamper the development of wall-layer models because it forces the calculations that use approximate boundary conditions to place the first grid point in the buffer region or in the lower reaches of the logarithmic layer and that use grids that are only a few hundred wall units in the streamwise and spanwise directions, which is in direct contradiction with the statistical assumption that underlies wall-layer modeling.

The renewed interest in the development of methodologies for the extension of LES to high Reynolds-number flows has so far raised more questions than it has answered. At present, reliable predictions cannot be expected except for fairly simple configurations. Based on the progress in modeling and numerical methodologies for LES over the last decade, however, one may hope that the next five years or so may bring substantial advancement in this area as well.

ACKNOWLEDGMENTS

The authors thank Professors P. Bradshaw, T.S. Lund, C. Meneveau, and Dr. P.R. Spalart for reviewing this manuscript. Prof. K.D. Squires kindly provided the velocity fields from the DES channel-flow calculations. The sustained support of the authors' work in this area by the Office of Naval Research (L.P. Purtell and C.E. Wark, Program Managers) is gratefully acknowledged.

LITERATURE CITED

Adrian RJ. 1979. Conditional eddies in isotropic turbulence. *Phys. Fluids* 22:2065–70

Akselvoll K, Moin P. 1995. Large eddy simulation of turbulent confined coannular jet and turbulent flow over a backward-facing step. *Rep.TF-63*, Thermosci. Div., Dept. Mech. Eng., Stanford Univ., Calif.

Baggett JS. 1998. On the feasibility of merging LES with RANS in the near-wall region of attached turbulent flows. In *Annu. Res.*

Briefs—1998, pp. 267–77. Center Turbul. Res., Stanford Univ., Calif.

Baggett JS, Nicoud F, Mohammadi B, Bewley T, Gullbrand J, Botella O. 2000. Suboptimal control based wall models for LES—including transpiration velocity. In *Proc. 2000 Summer Program*, pp. 331–42. Center Turbul. Res., Stanford Univ., Calif.

Bagwell TG, Adrian RJ, Moser RD, Kim J. 1993. Improved approximation of wall shear stress boundary conditions for large-eddy simulation. In *Near-wall Turbulent Flows*, ed. RMC So, CG Speziale, BE Launder, pp. 265–75. Amsterdam: Elsevier

Balaras E, Benocci C. 1994. Subgrid-scale models in finite-difference simulations of complex wall bounded flows. *AGARD CP 551*, pp. 2.1–2.5. Neuilly-Sur-Seine, France: AGARD

Balaras E, Benocci C, Piomelli U. 1995. Finite difference computations of high Reynolds number flows using the dynamic subgrid-scale model. *Theoret. Comput. Fluid Dyn.* 7:207–16

Balaras E, Benocci C, Piomelli U. 1996. Two-layer approximate boundary conditions for large-eddy simulations. *AIAA J.* 34:1111–19

Cabot WH. 1995. Large-eddy simulations with wall models. In *Annu. Res. Briefs—1995*, pp. 41–50. Center Turbul. Res., Stanford Univ., Calif.

Cabot WH. 1996. Near-wall models in large-eddy simulations of flow behind a backward-facing step. In *Annu. Res. Briefs—1996*, pp. 199–210. Center Turbul. Res., Stanford Univ., Calif.

Cabot WH, Jimenez J, Baggett JS. 1999. On wakes and near-wall behavior in coarse large-eddy simulation of channel flow with wall models and second-order finite difference methods. In *Annu. Res. Briefs—1999*, pp. 343–454. Center Turbul. Res., Stanford Univ., Calif.

Cabot WH, Moin P. 1999. Approximate wall boundary conditions in the large-eddy simulation of high Reynolds number flows. *Flow Turbul. Combust.* 63:269–91

Chapman DR. 1979. Computational aerodynamics, development and outlook. *AIAA J.* 17:1293–313

Deardorff JW. 1970. A numerical study of three-dimensional turbulent channel flow at large Reynolds numbers. *J. Fluid Mech.* 41: 453–80

Diurno GV, Balaras E, Piomelli U. 2001. Wall-layer models for LES of separated flows. In *Modern Simulation Strategies for Turbulent Flows*, ed. B Geurts, pp. 207–22. Philadelphia, PA: RT Edwards

Germano M, Piomelli U, Moin P, Cabot WH. 1991. A dynamic subgrid-scale eddy viscosity model. *Phys. Fluids A* 3:1760–65

Grötzbach G. 1987. Direct numerical and large eddy simulation of turbulent channel flows. In *Encyclopedia of Fluid Mechanics*, ed. NP Cheremisinoff, pp. 1337–91. West Orange, NJ: Gulf Publ.

Hoffman G, Benocci C. 1995. Approximate wall boundary conditions for large-eddy simulations. In *Advances in Turbulence V*, ed. R Benzi, pp. 222–28. Dordrecht: Kluwer

Johnston JP, Halleen RM, Lezius RK. 1972. Effect of spanwise rotation on the structure of two-dimensional fully developed turbulent channel flow. *J. Fluid Mech.* 56:533–57

Kaltenbach H-J, Fatica M, Mittal R, Lund TS, Moin P. 1999. Study of flow in a planar asymmetric diffuser using large-eddy simulation. *J. Fluid Mech.* 390:151–85

Kristoffersen R, Andersson HI. 1993. Direct simulation of low-Reynolds number turbulent flow in rotating channel. *J. Fluid Mech.* 256:163–97

Lamballais E, Métais O, Lesieur M. 1998. Spectral-dynamic model for large-eddy simulations of turbulent rotating channel flow. *Theoret. Comput. Fluid Dyn.* 12:149–77

Laufer J. 1950. Investigation of turbulent flow in a two-dimensional channel. *NACA TN 1053*. Washington, DC: Natl. Advis. Comm. Aeronaut.

Lesieur M, Métais O. 1996. New trends in large-eddy simulation of turbulence. *Annu. Rev. Fluid Mech.* 28:45–82

Mason PJ. 1994. Large-eddy simulation: a

critical review of the technique. *Q. J. Meteorol. Soc.* 120:1–26

Mason PJ, Callen NS. 1986. On the magnitude of the subgrid-scale eddy coefficient in large-eddy simulation of turbulent channel flow. *J. Fluid Mech.* 162:439–62

Mason PJ, Thomson DJ. 1992. Stochastic backscatter in large-eddy simulations of boundary layers. *J. Fluid Mech.* 242:51–78

Meneveau C, Katz J. 2000. Scale invariance and turbulence models for large-eddy simulation. *Annu. Rev. Fluid Mech.* 32:1–32

Moeng C-H. 1984. A large-eddy simulation model for the study of planetary boundary-layer turbulence. *J. Atmos. Sci.* 41:13

Moin P, Mahesh K. 1998. Direct numerical simulation: a tool in turbulence research. *Annu. Rev. Fluid Mech.* 30:539–78

Naguib AM, Wark CE. 1992. An investigation of wall-layer dynamics using a combined temporal and correlation technique. *J. Fluid Mech.* 243:541–60

Nicoud F, Bagget JS, Moin P, Cabot W. 2001. Large eddy simulation wall-modeling based on suboptimal control theory and linear stochastic estimation. *Phys. Fluids* 13:2968–84

Nikitin NV, Nicoud F, Wasistho B, Squires KD, Spalart PR. 2000. An approach to wall modeling in large-eddy simulations. *Phys. Fluids* 12:1629–32

Pao YH. 1965. Structure of turbulent velocity and scalar fields at large wave numbers. *Phys. Fluids* 8:1063–75

Piomelli U. 1999. Large-eddy simulation: achievements and challenges. *Prog. Aerosp. Sci.* 35:335–62

Piomelli U, Liu J. 1995. Large-eddy simulation of rotating channel flows using a localized dynamic model. *Phys. Fluids A* 7:839–48

Piomelli U, Moin P, Ferziger JH, Kim J. 1989. New approximate boundary conditions for large-eddy simulations of wall-bounded flows. *Phys. Fluids A* 1:1061–68

Porté-Agel F, Meneveau C, Parlange MB. 2000. A scale-dependent dynamics model for large-eddy simulation: application to a neutral atmospheric boundary layer. *J. Fluid Mech.* 415:261–84

Reynolds WC. 1990. The potential and limitations of direct- and large-eddy simulations. In *Whither Turbulence? Turbulence at the Crossroads*, ed. JL Lumley, pp. 313–42. Heidelberg: Springer

Robinson SK. 1991. Coherent motions in the turbulent boundary layer. *Annu. Rev. Fluid Mech.* 23:601–39

Schumann U. 1975. Subgrid-scale model for finite difference simulation of turbulent flows in plane channels and annuli. *J. Comput. Phys.* 18:376–404

Smagorinsky J. 1963. General circulation experiments with the primitive equations. I. The basic experiment. *Mon. Weather Rev.* 91:99–164

Spalart PR. 2000. Trends in turbulence treatments. *AIAA Paper 2000-2306*. Washington, DC: Am. Inst. Aeronaut. Astronaut.

Spalart PR, Allmaras SR. 1994. A one-equation turbulence model for aerodynamic flows. *Rech. Aérosp.* 1:5–21

Spalart PR, Jou WH, Strelets M, Allmaras SR. 1997. Comments on the feasibility of LES for wings and on a hybrid RANS/LES approach. In *Advances in DNS/LES*, ed. C Liu, Z Liu, pp. 137–48. Columbus, OH: Greyden

Strelets M. 2001. Detached-eddy simulation of massively separated flows. *AIAA Paper No. 2001-0879*. Washington, DC: Am. Inst. Aeronaut. Astronaut.

Sullivan P, McWilliams JC, Moeng C-H. 1994. A subgrid-scale model for large-eddy simulation of planetary boundary-layer flows. *Bound.-Layer Meteorol.* 71:247–76

Verzicco R, Mohd-Yusof J, Orlandi P, Haworth D. 2000. Large-eddy simulation in complex geometric configurations using boundary-body forces. *AIAA J.* 38:427–33

Wang M. 1999. LES with wall models for trailing-edge aeroacoustics. In *Annu. Res. Briefs—1999*, pp. 355–64. Center Turbul. Res., Stanford Univ., Calif.

Wang M. 2000. Dynamic-wall modeling for LES of complex turbulent flows. In *Annu.*

Res. Briefs—1999, pp. 241–50. Center Turbul. Res., Stanford Univ., Calif.

Wang M, Moin P. 2000. Computation of trailing-edge flow and noise using large-eddy simulation. *AIAA J.* 38:2201–9

Werner H, Wengle H. 1993. Large-eddy simulation of turbulent flow around a cube in a plane channel. In *Selected Papers from the 8th Symposium on Turbulent Shear Flows*, ed. F Durst, R Friedrich, BE Launder, U Schumann, JH Whitelaw, pp. 155–68. New York: Springer

Wilcox D. 2001. Turbulence modeling: an overview. *AIAA Paper No. 2001–0724*. Washington, DC: Am. Inst. Aeronaut. Astronaut.

Wu X, Squires KD. 1998. Prediction of the three-dimensional turbulent boundary layer over a swept bump. *AIAA J.* 36:505–14

Zhang C, Randall DA, Moeng C-H, Branson M, Moyer KA, Wang Q. 1996. A surface flux parameterization based on the vertically averaged turbulence kinetic energy. *Mon. Weather Rev.* 124:2521–36

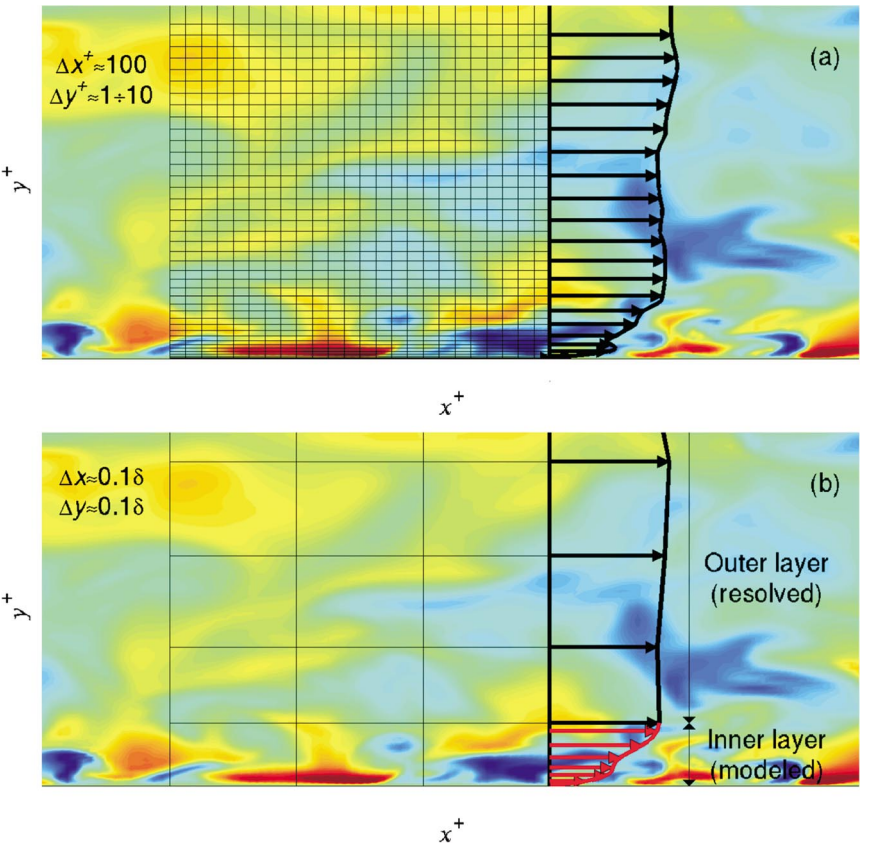

Figure 2 Sketch illustrating the wall-layer modeling philosophy. (*a*) Inner layer resolved. (*b*) Inner layer modeled.

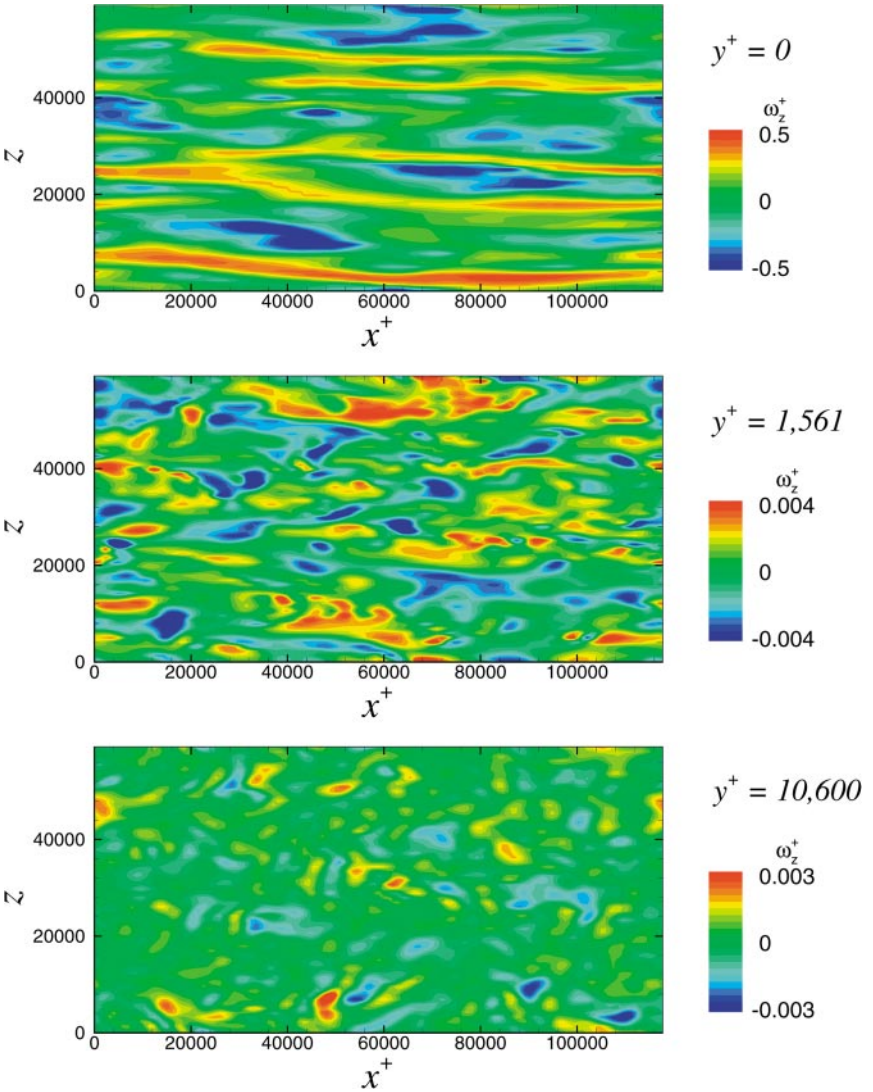

Figure 11 Spanwise vorticity fluctuations in plane-chanel flow. DES wall-layer model, $Re_\tau = 20{,}000$, fine calculation. $y^+ = 650$ is the interface between LES and RANS regions (K.D. Squires, personal communication).

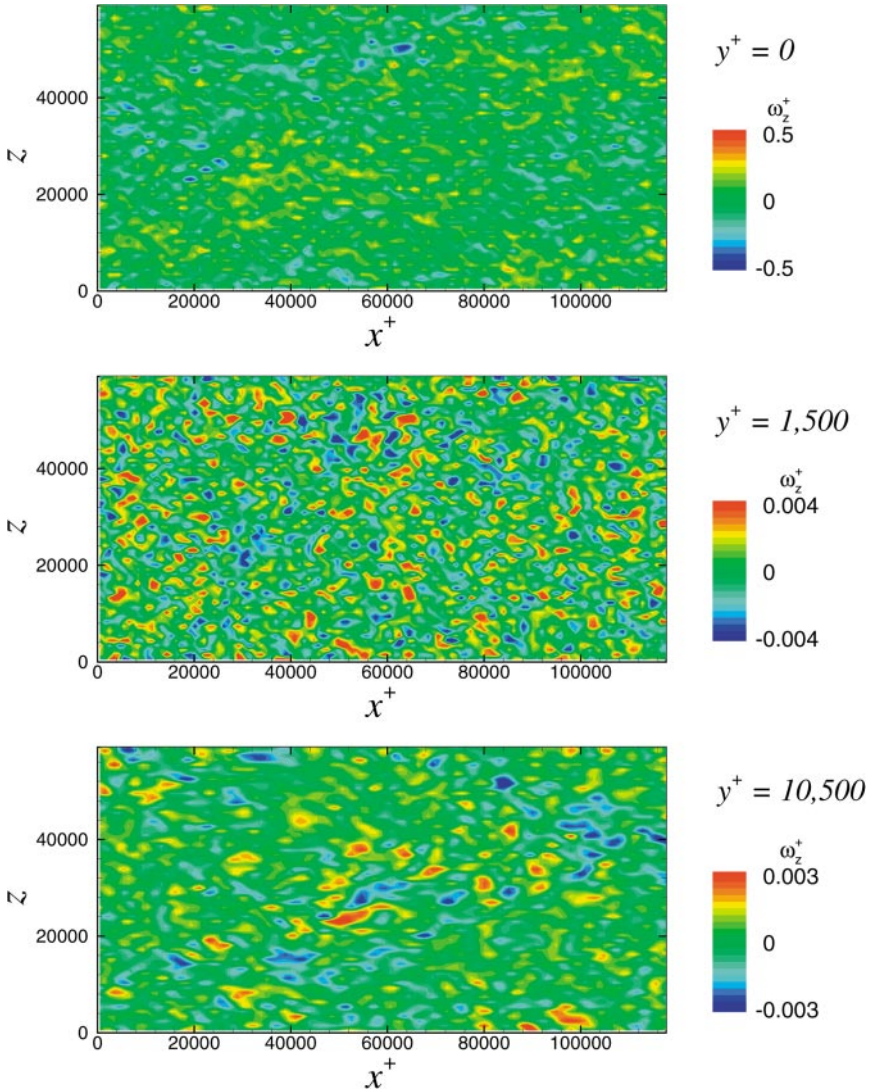

Figure 12 Spanwise vorticity fluctuations in plane-channel flow. Logarithmic-law wall-layer model (9–10) $Re_\tau = 20{,}000$. The first velocity point is at $y^+ = 500$.